

THE RHEALPIX DISCRETE GLOBAL GRID SYSTEM

ROBERT GIBB, ALEXANDER RAICHEV, AND MICHAEL SPETH

ABSTRACT. We extend the HEALPix discrete global grid system (DGGS) to ellipsoids of revolution, thereby broadening its possible applications. Elaborating on the work of Calabretta and Roukema [Mapping on the HEALPix grid, Monthly Notices of the Royal Astronomical Society 381 (2007), no. 2, 865–872.], we also rearrange the HEALPix map projection and build a new DGGS on top of it, which we call the rHEALPix DGGS. The rHEALPix DGGS has all the key features of the HEALPix DGGS, making it excellent for applications that require harmonic analysis. Additionally, its planar projection consists of horizontal-vertical aligned nested square grids, which are easy to understand and display. We present all the formulas and algorithms necessary for a basic implementation of the rHEALPix DGGS and link to our own open source implementation.

1. INTRODUCTION

A **discrete global grid** is a finite partition of the surface of an ellipsoid, which could be a sphere, along with a set of distinguished points, one point in each partition element. A partition element is called a **cell** and its unique associated point is called a **nucleus** in this paper*. A **discrete global grid system (DGGS)** is a sequence of discrete global grids, usually of increasingly finer resolution. DGGSs are used to store and analyze ellipsoidal spatial data to study celestial and planetary phenomena such as cosmic microwave background radiation and global warming [SWK03].

The HEALPix DGGS was introduced in [GHB⁺05] to study cosmic microwave background radiation and has the following key features:

- (i) It is hierarchical, congruent, aligned for odd values of an integer parameter N_{side} , and constant aperture, which makes it easy to implement with efficient data structures.
- (ii) At every resolution its grid cells have equal areas, which provide equal probabilities for statistical analyses.
- (iii) At each resolution its k nuclei lie on only $\Theta(\sqrt{k})$ parallels of latitude, which makes computing spherical harmonics fast.
- (iv) Its planar projection has low average angular and linear distortion.

In this paper we extend the HEALPix DGGS, which was initially defined only for spheres, so that:

- (v) It can be used on ellipsoids of revolution such as the WGS84 ellipsoid, which is also used by the Global Positioning System and most satellite-based sensors.

We do this while preserving features (i)–(iv), thereby broadening the possible applications of the HEALPix DGGS.

Elaborating on the work of [CR07, Section 3.1], we also rearrange the underlying HEALPix map projection into what we call the rHEALPix map projection and detail a

Date: 12 March 2013.

Key words and phrases. HEALPix, rHEALPix, discrete global grid system.

* We prefer the term ‘nucleus’ over the more common term ‘cell center’, because the latter can be misleading: a cell’s nucleus is often not its centroid.

DGGS for ellipsoids of revolution based upon it, which we call the rHEALPix DGGS. The rHEALPix DGGS also has features (i)–(v) and additionally:

- (vi) Its planar projection consists of horizontal-vertical aligned nested square grids, which are easy to understand and display.

So by the criteria 1, 2, 6, 8, 9, 12, and 14 of [KSWS99], the rHEALPix DGGS is a good choice of DGGS for storage and analysis of ellipsoidal spatial data and an especially good choice when harmonic analysis is required.

The rHEALPix DGGS can be construed as a mapping of an ellipsoid of revolution onto a regular polyhedron, namely a cube, followed by a symmetric hierarchical partitioning of the polyhedral faces along with a choice of nuclei, followed by the inverse mapping of the result back onto the ellipsoid. Thus the rHEALPix DGGS is an example of a geodesic DGGS, specifically a cubic geodesic DGGS [SWK03].

To the best of our knowledge, the only DGGSs satisfying properties (i)–(vi) are the rHEALPix DGGS and other variants based on rigid transformations of the HEALPix projection[†]. Three DGGSs that come close are the COBE DGGS [CO75, CG02], its variant [OL76, CG02] based on the quadrilateralized spherical cube projection, and a rotation and square partitioning of Snyder’s equal-area cubic projection [Sny92], all of which are cubic geodesic DGGS satisfying properties (i)–(ii) and (iv)–(vi) after minor adjustment[‡]. However all three fail (iii), because they have $\Theta(k)$ nucleus parallels.

Of course, in applications where features (i)–(vi) are not required, the rHEALPix DGGS might not be appropriate. For example, fluid flow models typically require grids with uniform adjacency, ones where all cells that share boundaries share edge boundaries. In that case, grids with hexagonal rather than quadrilateral cells are appropriate [SWK03, page 127].

Our implementations of the extended HEALPix and rHEALPix map projections can be found in the forthcoming release (after 4.8) of the PROJ.4 cartographic library, and our Python implementation of the rHEALPix DGGS can be found at Landcare Research’s git repository <http://code.scenzgrid.org/index.php/p/scenzgrid-py/>. Both of these implementations are open source and based upon the formulas and algorithms included in this paper.

2. DEFINING THE RHEALPIX DGGS

Choose a base ellipsoid of revolution, hereafter referred to as **the ellipsoid**, and place a geodetic longitude-latitude coordinate frame on it. For instance, the ellipsoid could be the WGS84 ellipsoid with the WGS84 coordinate frame. Let R_q denote the radius of the ellipsoid’s authalic sphere, the unique sphere having the same surface area as the ellipsoid. In the case of the WGS84 ellipsoid, $R_q = 6,374,581.4671$ m. For mathematical convenience, we measure all angles in radians and all lengths in meters unless indicated otherwise.

Extending the HEALPix DGGS from a sphere to the ellipsoid while preserving features (i)–(iv) is straightforward. Simply (a) map the ellipsoid onto its authalic sphere in the standard area-preserving fashion; (b) map the authalic sphere onto the plane with the

[†] As also mentioned in [CR07, Section 3], the HEALPix projection image can be rotated by 45° and then partitioned with horizontal-vertical aligned nested square grids to produce another cubic DGGS with features (i)–(vi). The drawback there, though, is that all parallels of latitude project to the plane at 45° angles, which can confuse human viewers. So we do not pursue that DGGS here.

[‡] Strictly speaking, the cells of the COBE DGGS have approximately but not exactly equal areas. It and its variant can be aligned by introducing an N_{side} parameter and both can be extended to ellipsoids of revolution in the same way we extend the HEALPix DGGS.

HEALPix projection; (c) define the usual HEALPix planar grid system; (d) map this grid system back to the ellipsoid by applying inverses. This process preserves features (i)–(iv) of the HEALPix DGGS, because the map in step (a) preserves local areas, sends meridians to meridians, parallels to parallels, and has low average distortion. For the mathematical details of the HEALPix projection, see Appendix A.

To define the rHEALPix DGGS, also follow process (a)–(d) but instead use a rearranged version of the HEALPix projection in (b) and a simpler horizontal-vertical aligned square grid system in (c). More specifically, for step (b) map the authalic sphere to the plane via the (n, s) -rHEALPix projection for some choice of integers $0 \leq n, s \leq 3$; see Figure 1(b). Just like the HEALPix projection, the (n, s) -rHEALPix projection is equiareal with area scaling factor $3\pi/8$. A map projection of an ellipsoid is called **equiareal** if there exists a constant $k > 0$ such that every region of area A on the ellipsoid projects to a region of area kA on the plane. In other words, equal areas on the ellipsoid map to equal areas on the plane. For the mathematical details of the rHEALPix projection, see Appendix B.

For step (c), recursively construct a sequence G_0, G_1, G_2, \dots of nested grids on the planar projection as follows. Let G_0 be the set of 6 squares of width $R_q\pi/2$ whose upper left vertices lie at $R_q(-\pi + n\pi/2, 3\pi/4)$, $R_q(-\pi, \pi/4)$, $R_q(-\pi/2, \pi/4)$, $R_q(0, \pi/4)$, $R_q(\pi/2, \pi/4)$, and $R_q(-\pi + s\pi/2, -\pi/4)$. Choose an integer $N_{\text{side}} \geq 2$, and for each integer $i \geq 0$ let G_{i+1} be the grid obtained by refining each square of grid G_i into $N_{\text{side}} \times N_{\text{side}}$ isomorphic sub-squares. Then each grid G_i comprises $6 \cdot N_{\text{side}}^{2i}$ isomorphic square cells, each having side length $R_q(\pi/2)N_{\text{side}}^{-i}$ and area $R_q^2(\pi^2/4)N_{\text{side}}^{-2i}$. Define the nucleus of each cell to be its centroid. Call each planar grid G_i the **(n, s) -rHEALPix planar grid of resolution i** , and call the nested sequence $G := (G_0, G_1, G_2, \dots)$ of planar grids the **(n, s) -rHEALPix planar grid hierarchy**; see the left side of Figure 2. Strictly speaking, G is not a DGGS, since each of its grids partition a planar projection of the ellipsoid rather than the ellipsoid itself.

For step (d), map each planar grid G_i and its nuclei set back to the ellipsoid via the inverse (n, s) -rHEALPix projection, call the resulting ellipsoidal grid G'_i the **(n, s) -rHEALPix ellipsoidal grid of resolution i** , and call the nested sequence $G' := (G'_0, G'_1, G'_2, \dots)$ of ellipsoidal grids the **(n, s) -rHEALPix ellipsoidal grid hierarchy**; see the right side of Figure 2. This latter hierarchy is the **(n, s) -rHEALPix DGGS**. Each grid G'_i comprises $6 \cdot N_{\text{side}}^{2i}$ cells of four different shapes types detailed in Section 4. All resolution i cells have equal area, namely $R_q^2(\pi^2/4)N_{\text{side}}^{-2i}/(3\pi/8) = R_q^2(2\pi/3)N_{\text{side}}^{-2i}$, because the (n, s) -rHEALPix map projection is equiareal with area scaling factor $3\pi/8$. Note that the nucleus of an ellipsoidal cell, being the inverse image of the nucleus of its corresponding planar cell, is in general not its ellipsoidal centroid; see Section 7 for a calculation of the centroid. Note also that for the area $R_q^2(2\pi/3)N_{\text{side}}^{-2i}$ of an ellipsoidal cell to be at most A square meters, the resolution resolution i must be at least $\lceil \log(R_q^2(2\pi/3)A^{-1})/(2 \log N_{\text{side}}) \rceil$. For example, for $N_{\text{side}} = 3$, the cells of G'_i have area no greater than one square meter when $i \geq 15$; G'_{15} has $6 \cdot 9^{15} = 1,235,346,792,567,894$ cells. See Table 1

Besides being hierarchical and recursive, the hierarchies G and G' are both **congruent**, that is, each resolution i cell is a union of resolution $i + 1$ cells; when N_{side} is odd the hierarchies G and G' are both **aligned**, that is, each resolution i cell nucleus is the nucleus of a resolution $i + 1$ cell; the hierarchies G and G' both have a **constant aperture** of N_{side}^2 , that is, each resolution i cell has N_{side}^2 times the area of its resolution $i + 1$ subcells.

As a running example throughout this paper we use the $(0, 0)$ -rHEALPix DGGS with $N_{\text{side}} = 3$. The choice of $N_{\text{side}} = 3$ produces aligned hierarchies with the greatest number of resolutions per fixed maximum areal resolution.

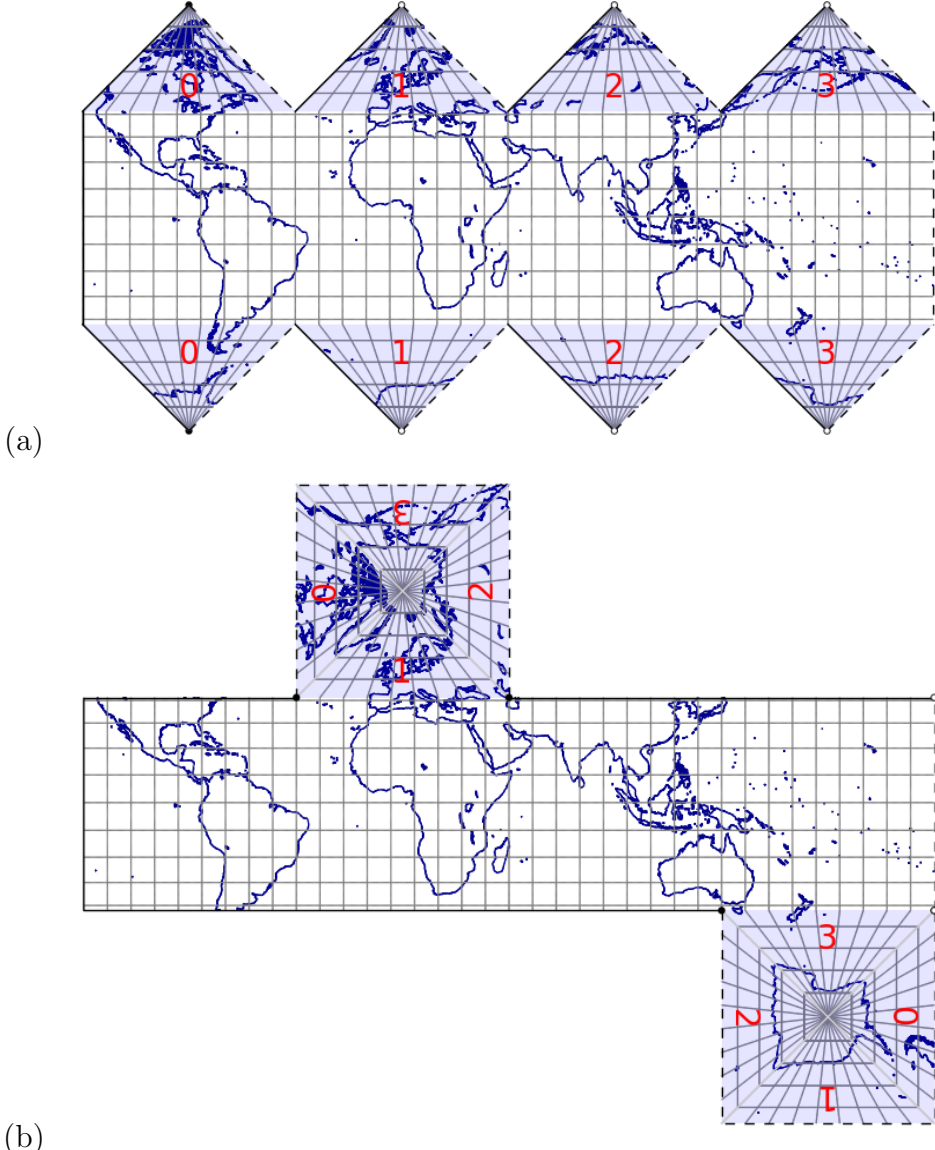


FIGURE 1. The (a) HEALPix and (b) (1, 3)-rHEALPix projections of the WGS84 ellipsoid with a 10° graticule. To illustrate some of the (r)HEALPix projection options, the prime meridian has been shifted to 50° east longitude to move the polar triangle boundary cuts to sparsely populated regions, and the polar triangles have been rearranged into the (1, 3) position for a better view of Europe and New Zealand.

3. CELL ID

For reference we assign unique names to the cells of the planar hierarchy G that are shared with the corresponding cells of the ellipsoidal hierarchy G' . These names echo the tree structure of the hierarchies and are defined as follows.

Let Γ be the set of all strings beginning with one of the letters N, O, \dots, S and followed by zero or more of the integers $0, 1, \dots, N_{\text{side}}^2 - 1$. In other words, Γ is the regular language $(N|O|\cdots|S)(0|1|\cdots|(N_{\text{side}}^2 - 1))^*$. The **identifier (ID)** of a cell c from G , denoted $\text{ID}(c)$, is the string in Γ defined by the following recursive procedure. Assign the cells of G_0 the IDs N, O, P, Q, R, S from top to bottom and left to right. In particular, cell N contains

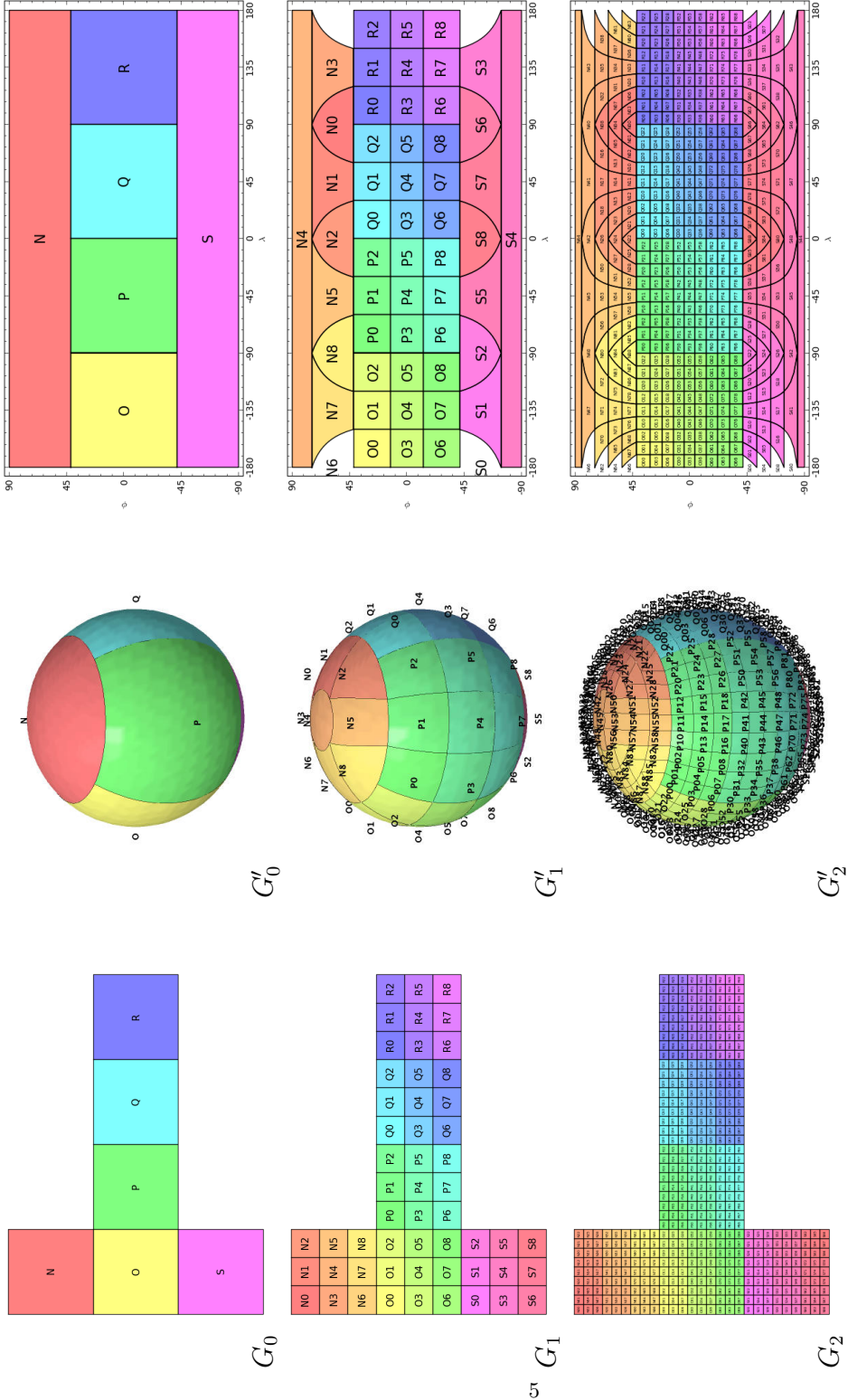


FIGURE 2. The first three planar and ellipsoidal grids for the $(0,0)$ -rHEALPix map projection with $N_{\text{side}} = 3$ and cells labeled with their IDs. For longitude-latitude reference, equirectangular projections of the ellipsoidal grids have also been included.

resolution	cell area (m ²)	$\sqrt{\text{cell area}}$ (m)	number of cells
0	8.5E+13	9.2E+06	6
1	9.5E+12	3.1E+06	54
2	1.1E+12	1E+06	4.9E+02
3	1.2E+11	3.4E+05	4.4E+03
4	1.3E+10	1.1E+05	3.9E+04
5	1.4E+09	3.8E+04	3.5E+05
6	1.6E+08	1.3E+04	3.2E+06
7	1.8E+07	4.2E+03	2.9E+07
8	2E+06	1.4E+03	2.6E+08
9	2.2E+05	4.7E+02	2.3E+09
10	2.4E+04	1.6E+02	2.1E+10
11	2.7E+03	52	1.9E+11
12	3E+02	17	1.7E+12
13	33	5.8	1.5E+13
14	3.7	1.9	1.4E+14
15	0.41	0.64	1.2E+15

TABLE 1. Approximate cell area and approximate number of cells for successive grids of the $N_{\text{side}} = 3$ ellipsoidal rHEALPix grid hierarchy on the WGS84 ellipsoid.

the projection of the north pole and cell S contains the projection of the south pole. For each resolution i cell with ID s assign its N_{side}^2 resolution $i + 1$ subcells the IDs $s0, s1, \dots, s(N_{\text{side}}^2 - 1)$ from top to bottom and left to right; see Figures 2 and 3.

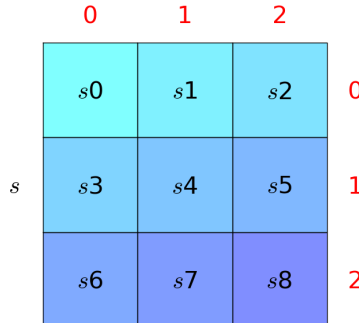


FIGURE 3. An $N_{\text{side}} = 3$ rHEALPix planar cell at resolution i and with ID s . Its $N_{\text{side}}^2 = 9$ resolution $i + 1$ subcells are labeled with their IDs and their row and column numbers are highlighted in red.

Henceforth we will refer to cells by their IDs and sometimes blur the distinction between numbers and strings when the context is clear.

4. CELL SHAPE AND DISTRIBUTION

Consider the grids G_i and G'_i .

The planar grid G_i comprises $6 \cdot N_{\text{side}}^{2i}$ axis-aligned isomorphic square cells, each of side length $R_q(\pi/2)N_{\text{side}}^{-i}$. In the **equatorial region** of the plane, the region $|y| \leq R_q\pi/4$, there are $4 \cdot N_{\text{side}}^{2i}$ axis-aligned isomorphic square cells arranged along N_{side}^i rows and

$4 \cdot N_{\text{side}}^i$ columns. In the **polar region** of the plane, the non-equatorial region, there are $2 \cdot N_{\text{side}}^{2i}$ square cells. Half of these lie in the north polar region ($y > R_q\pi/4$) arranged along N_{side}^i rows and N_{side}^i columns, and the other half of these lie in the south polar region ($y < -R_q\pi/4$) arranged along N_{side}^i rows and N_{side}^i columns. The columns in the north and south coincide when $n = s$ in the (n, s) -rHEALPix projection used.

The ellipsoidal grid G'_i is symmetric with respect to a $\pi/2$ longitudinal rotation or a $\pi/2$ latitudinal rotation of the ellipsoid and comprises $6 \cdot N_{\text{side}}^{2i}$ cells of equal areas and of four different shape types. Except for the two cells centered at the poles, each cell has its northern edge/vertex lying on one parallel and its southern edge/vertex lying on another parallel.

In the equatorial region of the ellipsoid, the region of authalic latitudes of magnitude at most $\arcsin(2/3) \approx 41.8^\circ$, there are $4 \cdot N_{\text{side}}^{2i}$ cells, all of which are ellipsoidal quadrangles with longitude-latitude-aligned edges. We call an ellipsoidal cell of this shape a **quad cell**; see cell $P1$ in Figure 2 for instance. Quads have IDs of the form $(O|P|Q|R)(0|1|\cdots|N_{\text{side}}^2 - 1)^*$, in terms of regular expressions. The nuclei of quad cells are spread unequally in latitude across N_{side}^i parallels, and on each such parallel there are $4 \cdot N_{\text{side}}^i$ cell nuclei spread equally in longitude.

In the polar region of the ellipsoid, the non-equatorial region, there are $2 \cdot N_{\text{side}}^{2i}$ cells of three different shape types, or two different shape types if N_{side} is even. Half of these cells lie in the north polar region and the other lie in the south polar region. Since these two polar grid regions are isomorphic, let us just consider the north polar region. In that region, if N_{side} is odd, then there is one cell whose nucleus lies at the north pole and whose shape is an ellipsoidal cap, that is, the boundary of the cell lies along a single parallel. We call an ellipsoidal cell of this shape a **cap cell**; see cell $N4$ in Figure 2 for instance. Caps have IDs of the form $(N|S)((N_{\text{side}}^2 - 1)/2)^*$. If N_{side} is even, then there are no cap cells.

The remaining $N_{\text{side}}^{2i} - 1$ north polar cells, or N_{side}^{2i} if N_{side} is even, come in two different shapes. A cell whose nucleus lies off the poles and at longitude $-\pi, -\pi/2, 0$, or $\pi/2$ (the longitudes of the diagonal and antidiagonal of planar cells N and S) has three edges, one of which lies on a parallel and the other two of which have equal lengths and converge polewards to a point. We call an ellipsoidal cell of this shape a **dart cell**; see cell $N2$ in Figure 2 for instance. Darts have IDs of the form $(N|S)((0|(N_{\text{side}} + 1)|2(N_{\text{side}} + 1)|\cdots|(N_{\text{side}} - 1)(N_{\text{side}} + 1))^+ | ((N_{\text{side}} - 1)|2(N_{\text{side}} - 1)|\cdots|N_{\text{side}}(N_{\text{side}} - 1))^+)$, excluding cap cell IDs. All other polar cells are ellipsoidal quadrangles that have their northern and southern edges lying on two parallels. We call an ellipsoidal cell of this shape a **skew quad cell**; see cell $N5$ in Figure 2 for instance. The nuclei of the northern dart cells and skew quad cells are spread unequally in latitude across $\lfloor N_{\text{side}}^i/2 \rfloor$ parallels with $4(N_{\text{side}}^i - 2j + 1)$ cell nuclei spread equally in longitude along each such parallel band $j \in \{1, \dots, \lfloor N_{\text{side}}^i/2 \rfloor\}$, where the band numbers increase polewards. Of these $4(N_{\text{side}}^i - 2j + 1)$ cells, 4 are dart cells and the remaining $4(N_{\text{side}}^i - 2j)$ are skew quad cells. So in the north polar in total there are $4\lfloor N_{\text{side}}^i/2 \rfloor$ dart cells and $(N_{\text{side}}^i - 1)^2$ skew quad cells, or $(N_{\text{side}}^i - 1)^2 - 1$ skew quad cells if N_{side} is even.

Notice that the nuclei of the $k := 6 \cdot N_{\text{side}}^{2i}$ ellipsoidal cells lie along only $2N_{\text{side}}^i - 1$ (non-pole) parallels if N_{side} is odd and $2N_{\text{side}}^i$ parallels if N_{side} is even, that is, $\Theta(\sqrt{k})$ parallels. This square root dependence also holds for the HEALPix DGGS. Indeed, it was designed into it so that computing spherical harmonics is relatively fast. Computing spherical or ellipsoidal harmonics on the ellipsoid involves computing Legendre polynomials at each nucleus parallel, which is recursive and slow, and so the fewer the parallels, the faster the

computation [GHB⁺05, Section 5] [Nes11]. For comparison, the COBE DGGS used by NASA before HEALPix has $\Theta(k)$ nucleus parallels at each grid resolution.

5. CELL BOUNDARIES AND NEIGHBORS

Because the image of an rHEALPix map projection does not completely contain its boundary (see Figure 1), the cells of G and G' cannot contain all their edges. Let us declare somewhat arbitrarily that cells N and S contain none of their edges and that cells $O-R$ contain their left, top, and bottom edges. Recursing, let us declare that each child cell contains its left and top edges unless it shares a boundary with its parent, in which case it inherits its parent's boundary. For example, cell $N5$ contains its left and top edges, and cell $N0$ contains none of its edges. In our drawings of cells we ignore these subtleties of boundary by representing all boundaries with solid lines.

Every ellipsoidal cell c shares an edge with four other cells, which we call the **neighbors** of c . Additionally, c shares a boundary point with three or four other cells, depending on whether c is or is not a dart, respectively. For simplicity, we do not consider these three or four other adjacent cells neighbors of c . For a cell on the boundary between the equatorial and polar region of the ellipsoid, the names of its neighboring cells depend on the parameters n and s of the chosen (n, s) -rHEALPix projection, that is, on how the polar triangles of the HEALPix map projection are combined. For example, in the $(0, 0)$ -rHEALPix DGGS with $N_{\text{side}} = 3$, the neighbors of $P0$ are $N8, O2, P3$, and $P1$. In the $(0, 2)$ -rHEALPix DGGS with $N_{\text{side}} = 3$, the neighbors of $P0$ are $N8, O2, P3$, and $P1$.

The cell adjacency structure of the ellipsoidal hierarchy G' induces a cell adjacency structure on the planar hierarchy G that can be visualized by folding G_0 into a cube along its cell edges, and this is how the rHEALPix DGGS can be construed as a geodesic DGGS; see Figure 4.

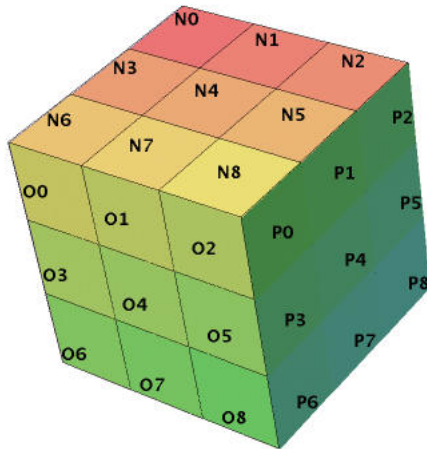


FIGURE 4. The cell adjacency structure of G_1 for the $(0, 0)$ -rHEALPix map projection with $N_{\text{side}} = 3$.

6. CELL VERTICES AND NUCLEUS

From a planar cell's ID we can compute its four vertices and nucleus as follows. For a string s of length k , let $s[i]$ denote the character of s at index i , where $0 \leq i < k$, and let

$s[i:]$ denote the string $s[i]s[i+1]\dots s[k-1]$. Given a digit in $\{0, 1, \dots, N_{\text{side}}^2 - 1\}$, let the **row ID** and **column ID** of the digit be its row and column index in the $N_{\text{side}} \times N_{\text{side}}$ subcell matrix of Figure 3. For example, for $N_{\text{side}} = 3$ we have $\text{rowID}(5) = 1$ and $\text{colID}(5) = 2$. Notice that the row and column IDs of a digit can be obtained from the base N_{side} expansion of the digit: $5 = (12)_3$. Given a letter in $\{N, O, \dots, S\}$, let its row and column ID be the letter itself. Let the row ID of a cell be the concatenation of the row IDs of its individual ID characters, and let the column ID of a cell be defined analogously. For example, for $N_{\text{side}} = 3$ we have $\text{rowID}(Q517) = Q102$ and $\text{colID}(Q517) = Q211$.

The last digit of a cell's ID determines the cell's upper left vertex relative to its parent cell's upper left vertex[§]. For example, for $N_{\text{side}} = 3$ consider the planar cell $s5$ of width w . The last digit of its ID is $5 = (12)_3$, and the cell lies $1 \cdot w$ down and $2 \cdot w$ right from the upper left vertex of its parent cell s . In general, for a cell sa of resolution at least 1 and with last digit a , we have

$$\text{ul}(sa) = \text{ul}(s) + w(\text{colID}(a), -\text{rowID}(a)),$$

where w is the width of cell sa and $\text{ul}(t)$ denotes the coordinates of the upper left vertex of cell t . Recursing on this formula and recalling that a cell of resolution i has width $(R_q\pi/2)N_{\text{side}}^{-i}$, we deduce that the upper left vertex of a resolution r planar cell with ID s is

$$\text{ul}(s) = \text{ul}(s[0]) + (R_q\pi/2) \sum_{i=1}^r N_{\text{side}}^{-i} (\text{colID}(s[i]), -\text{rowID}(s[i])),$$

Alternatively we could write the x and y coordinates of $\text{ul}(s)$, respectively, as

$$\begin{aligned} \text{ul}(s)_x &= \text{ul}(\text{colID}(s)[0])_x + (R_q\pi/2)(0.\text{colID}(s)[1:])_{N_{\text{side}}} \\ \text{ul}(s)_y &= \text{ul}(\text{rowID}(s)[0])_y - (R_q\pi/2)(0.\text{rowID}(s)[1:])_{N_{\text{side}}} \end{aligned}$$

For example, for $N_{\text{side}} = 3$ the upper left vertex of cell $Q517$ is

$$\begin{aligned} \text{ul}(P517)_x &= \text{ul}(P)_x + (R_q\pi/2)(0.211)_3 = R_q[-\pi/2 + (\pi/2)(2/3 + 1/9 + 1/27)] \\ \text{ul}(P517)_y &= \text{ul}(P)_y - (R_q\pi/2)(0.102)_3 = R_q[\pi/4 - (\pi/2)(1/3 + 2/27)]. \end{aligned}$$

From the upper left vertex coordinates (x, y) of a planar cell and from its width w , we can then compute the coordinates of its remaining vertices and nucleus.

$$\begin{aligned} \text{upper left vertex} &: (x, y) \\ \text{upper right vertex} &: (x + w, y) \\ \text{lower left vertex} &: (x, y - w) \\ \text{lower right vertex} &: (x + w, y - w) \\ \text{nucleus} &: (x + w/2, y - w/2). \end{aligned}$$

Projecting these vertices onto the ellipsoid produces the vertices of the corresponding ellipsoidal cell, if it is a quad cell or a skew quad cell. If the ellipsoidal cell is a dart or a cap cell, respectively, one or four of the projected points will be non-vertex boundary points. Projecting the nucleus of a planar cell onto the ellipsoid produces the nucleus of the corresponding ellipsoidal cell by definition.

[§] Notice that a cell might not contain its upper left vertex since it lies on the cell's boundary. For example, cell N does not contain its upper left vertex.

7. CELL CENTROID

By definition, the centroid of a planar cell is its nucleus, and projecting this nucleus back onto the ellipsoid yields the nucleus of the corresponding ellipsoidal cell. In general, however, the centroid of an ellipsoidal cell is not its nucleus. In other words, cell nuclei are preserved under the rHEALPix projection but centroids are not. We can compute the centroid of an ellipsoidal cell by integration and symmetry as follows.

Let r denote an rHEALPix map projection of the ellipsoid and observe that the average value of a real function $f(\lambda, \phi)$ on an ellipsoidal cell c is

$$\begin{aligned} \frac{1}{\text{area of } c} \iint_c f dS &= \frac{1}{\text{area of } c} \iint_{r[c]} (f \circ r^{-1})(x, y) \frac{8}{3\pi} dx dy \\ &= \frac{1}{\text{area of } r[c]} \iint_{r[c]} (f \circ r^{-1})(x, y) dx dy \end{aligned}$$

when parametrized by planar coordinates (x, y) . The factor $8/(3\pi)$ is the area scaling factor of r^{-1} , which is the reciprocal of the area scaling factor of r , and $r[c]$ is the planar projection of c . Applying this average value formula to the longitude $f(\lambda, \phi) = \lambda$ and latitude $f(\lambda, \phi) = \phi$ functions gives the coordinates $(\bar{\lambda}, \bar{\phi})$ of the centroid of cell c :

$$\begin{aligned} \bar{\lambda} &= w^{-2} \int_{y_1}^{y_2} \int_{x_1}^{x_2} r_\lambda^{-1}(x, y) dx dy \\ \bar{\phi} &= w^{-2} \int_{y_1}^{y_2} \int_{x_1}^{x_2} r_\phi^{-1}(x, y) dx dy, \end{aligned}$$

where $x_1 < x_2$ and $y_1 < y_2$ are the respective x and y extremes of the planar cell $r[c]$, $w = x_2 - x_1 = y_2 - y_1$ is its width, and r_λ^{-1} and r_ϕ^{-1} are the longitude and latitude components of r^{-1} , respectively.

For several ellipsoidal cell shapes we can skirt these integrals. By symmetry the centroid of every cap cell is its nucleus, namely $(-\pi, \pm\pi/2)$. Since every quad cell is longitude-latitude aligned, its centroid is the average of its two longitudinal extremes and the average of its two latitudinal extremes. In particular, the longitude of its centroid is the longitude of its nucleus. Also, every dart cell is bisected by a meridian, and so the longitude of its centroid is the longitude of its nucleus. The following table summarizes these observations with (λ_n, ϕ_n) denoting the cell's nucleus.

ellipsoidal cell	$\bar{\lambda}$	$\bar{\phi}$
cap	λ_n	ϕ_n
quad	λ_n	$(\phi(x_1, y_1) + \phi(x_1, y_2))/2$
dart	λ_n	$w^{-2} \int_{y_1}^{y_2} \int_{x_1}^{x_2} r_\phi^{-1} dx dy$
skew quad	$w^{-2} \int_{y_1}^{y_2} \int_{x_1}^{x_2} r_\lambda^{-1} dx dy$	$w^{-2} \int_{y_1}^{y_2} \int_{x_1}^{x_2} r_\phi^{-1} dx dy$

Note that from a cell's ID we can compute x_1 , x_2 , y_1 , y_2 , w , λ_n , and ϕ_n by the method in Section 6.

The integral for $\bar{\lambda}$ for a skew quad cell can be computed exactly. This is most easily done by considering the HEALPix projection of the cell and using the formula for the

longitude component of the inverse HEALPix projection given in Appendix A:

$$\begin{aligned}
\bar{\lambda} &= w^{-2} \int_{y_1}^{y_2} \int_{x_1}^{x_2} \left(x_c + \frac{x/R_q - x_c}{2 - 4y/(\pi R_q)} \right) dx dy \\
&= w^{-2} \left[[I(x, y)]_{x_1, y_1}^{x_2, y_2} \right] \\
&= w^{-2} (I(x_2, y_2) - I(x_1, y_2) - I(x_2, y_1) + I(x_1, y_1)) \\
I(x, y) &= \frac{\pi}{8} x (2R_q x_c - x) \log \left(1 - \frac{2y}{\pi R_q} \right) + x_c xy \\
x_1 &= x_0 - w/2 \\
x_2 &= x_0 + w/2 \\
y_1 &= |y_0| - w/2 \\
y_2 &= |y_0| + w/2 \\
x_c &= -\frac{3\pi}{4} + \frac{\pi}{2} \left\lfloor \frac{2(x_0/R_q + \pi)}{\pi} \right\rfloor \\
(x_0, y_0) &= \text{the HEALPix projection of the cell's nucleus.}
\end{aligned}$$

The integral for $\bar{\phi}$ for a skew quad cell or a dart cell, however, must be computed approximately/numerically, because there is no closed form formula for $r_\phi^{-1}(x, y)$, because there is no closed form formula for latitude in terms of authalic latitude; see Appendix A.3.

8. CELL FROM POINT

Given a point (x, y) in the rHEALPix planar image and an integer $i \geq 0$, we can compute the ID of the resolution i cell that contains (x, y) as follows. First compute by cases the resolution 0 cell c containing (x, y) . Then compute the horizontal and vertical distances from (x, y) to $\text{ul}(c)$:

$$(\Delta x, \Delta y) := (|\text{ul}(c)_x - x|, |\text{ul}(c)_y - y|).$$

Then find out how far along the width $R_q\pi/2$ of c lie Δx and Δy by computing the base N_{side} expansions $(0.s)_{N_{\text{side}}}$ and $(0.t)_{N_{\text{side}}}$ of $\Delta x/(R\pi/2)$ and $\Delta y/(R\pi/2)$, respectively. Truncating s and t at i digits then gives the column and row IDs, respectively, of the resolution i cell d containing (x, y) :

$$\text{ID}(d) = \text{ID}(c)(N_{\text{side}}t[0] + s[0])(N_{\text{side}}t[1] + s[1]) \cdots (N_{\text{side}}t[l] + s[l]).$$

We can do the same for points on the ellipsoid by projecting them into the plane and then carrying out the computation above.

9. CELL FROM REGION

Given a region A in an rHEALPix planar image that is bounded by an axis-aligned rectangle specified by, say, upper left and lower right vertices u and v , respectively, we can compute the smallest cell c wholly containing A , if it exists, as follows. For i from 0 to ∞ , compute the IDs of the resolution i cell containing u and the resolution i cell containing v , and halt at the first index r at which the two IDs disagree. The longest (length r) common prefix of these two IDs will be the ID of c . In case the longest common prefix is the empty string, then no cell entirely contains the region A .

We can use the same analysis for regions on the ellipsoid bounded by an longitude-latitude aligned ellipsoidal quadrangle by first projecting the quadrangle into the plane, calculating its axis-aligned bounding rectangle, and then proceeding as above.

10. CONCLUSION

We have now detailed enough of the rHEALPix DGGS for a basic implementation. As we have seen through properties (i)–(vi) enumerated in Section 1, the rHEALPix DGGS is a good choice of DGGS for the storage and analysis of spatial data on an ellipsoid of revolution, especially when harmonic analysis is required.

No single DGGS is ideal for all tasks, however [KSWS99], and the rHEALPix DGGS is no exception. As we mentioned in the introduction, it is not ideal in applications that require grids with uniform adjacency. We also suspect that it is not ideal in applications that require near equidistance of cell nuclei or extreme cell compactness. In that case, grids with triangular or hexagonal cells might be better [GKWS08]. In future work we would like to explore this suspicion by computing nuclei spacing and compactness metrics for the rHEALPix DGGS and comparing them with other DGGSs.

ACKNOWLEDGEMENTS

We thank Kevin Sahr and Martin Lambers for reading an early draft of this paper and offering constructive comments that have improved its quality.

REFERENCES

- [BS95] Lev M. Bugayevskiy and John P. Snyder, *Map projections: A reference manual*, Taylor Francis, 1995.
- [CG02] M. R. Calabretta and E. W. Greisen, *Representations of celestial coordinates in FITS*, Astronomy & Astrophysics **395** (2002), 1077–1122.
- [CO75] F. K. Chan and E. M. O’Neill, *Feasibility study of a quadrilateralized spherical cube earth data base*, computer sciences corporation, Tech. Report 2-75, Monterey, California: Environmental Prediction Research Facility, 1975.
- [CR07] Mark R. Calabretta and Boudewijn F. Roukema, *Mapping on the healpix grid*, Monthly Notices of the Royal Astronomical Society **381** (2007), no. 2, 865–872.
- [Eul78] Leonhard Euler, *De repraesentatione superficieis sphaericae super plano*, Acta Academiae Scientiarum Imperialis Petropolitinae (1778).
- [GG07] D. M. Goldberg and J. R. Gott III, *Flexion and skewness in map projections of the earth.*, Cartographica **42** (2007), 297–318.
- [GHB⁺05] K. M. Gorski, E. Hivon, A. J. Banday, B. D. Wandelt, F. K. Hansen, M. Reinecke, and M. Bartelman, *Healpix – a framework for high resolution discretization, and fast analysis of data distributed on the sphere*, The Astrophysical Journal **622** (2005), 759.
- [GKWS08] M. J. Gregory, A. J. Kimerling, D. White, and K. Sahr, *A comparison of intercell metrics on discrete global grid systems*, Computers, Environment and Urban Systems **32** (2008), 188–203.
- [KSWS99] Jon A. Kimerling, Kevin Sahr, Denis White, and Lian Song, *Comparing geometrical properties of global grids*, Cartography and Geographic Information Science **26** (1999), no. 4, 271–287.
- [Nes11] Otakar Nesvadba, *Nothing to fear from ellipsoidal harmonics*, European Geosciences Union General Assembly 2011 (Vienna, Austria), 2011.
- [OL76] E. M. O’Neill and R. E. Laubscher, *Extended studies of the quadrilateralized spherical cube earth data base*, Tech. Report 3-76, Computer Sciences Corp Silver Spring Md System Sciences Div, 1976.
- [Sny87] J. P. Snyder, *Map projections—a working manual*, U.S. Geological Survey professional paper, U.S. G.P.O., 1987.
- [Sny92] ———, *An equal-area map projection for polyhedral globes*, Cartographica **29** (1992), 10–21.

[SWK03] Kevin Sahr, Denis White, and A. Jon Kimerling, *Geodesic Discrete Global Grid Systems*, Cartography and Geographic Information Science **30** (2003), 121–134.

APPENDIX A. THE HEALPix PROJECTION

The HEALPix map projection of a given sphere is the $H = 4, K = 3$ member of an infinite family (parametrized by positive integers H and K) of map projections of the sphere. As observed in [CR07], it is the hybrid of a rescaled Lambert cylindrical equal area projection on equatorial latitudes $|\phi| \leq \phi_0 := \arcsin(2/3)$ and a 4-times interrupted Collignon projection on polar latitudes $|\phi| > \phi_0$; see Figure 1(a).

Some of its features are:

- (i) It is an equiareal projection with area scaling factor $3\pi/8$ and low average angular and linear distortion.
- (ii) Parallels of latitude project to horizontal lines.
- (iii) A parallel of latitude uniformly divided projects to a horizontal line uniformly divided.
- (iv) Meridians of longitude project to vertical lines in the equatorial region and lines converging polewards in the polar region.

A.1. Formulas for the Sphere. Let $\mathbb{S}_R^2 \subset \mathbb{R}^3$ denote the sphere of radius R centered at the origin. By a map projection of the sphere, we mean an injective function from \mathbb{S}_R^2 to the plane \mathbb{R}^2 . In cartography, points on the sphere are usually described in terms of their longitude and geodetic latitude, that is, via the bijective parametrization $p : D \rightarrow \mathbb{S}_R^2$ defined by

$$p(\lambda, \phi) = R(\cos \lambda \cos \phi, \sin \lambda \cos \phi, \sin \phi),$$

where $D = [-\pi, \pi) \times (-\pi/2, \pi/2) \cup \{(-\pi, \pi/2), (\pi, \pi/2)\}$. Specifying an injective function $f : D \rightarrow \mathbb{R}^2$, which we call a **signature function**, then uniquely determines a map projection $f \circ p^{-1}$ of the sphere.

The signature function of the HEALPix map projection is $h_R := \bar{R} \circ h_1$, where

$$\begin{aligned} h_1(\lambda, \phi) &= \begin{cases} (\lambda, \frac{3\pi}{8} \sin \phi) & \text{if } |\phi| \leq \phi_0 \\ (\lambda_c + (\lambda - \lambda_c)\sigma, \operatorname{sgn}(\phi)\frac{\pi}{4}(2 - \sigma)) & \text{else} \end{cases} \\ \sigma &= \sqrt{3(1 - |\sin \phi|)} \\ \lambda_c &= -\frac{3\pi}{4} + \frac{\pi}{2} \left\lfloor \frac{2(\lambda + \pi)}{\pi} \right\rfloor \\ \bar{R}(x, y) &= (Rx, Ry). \end{aligned}$$

See Figure 5(a). Consequently, its inverse is $h_R^{-1} = h_1^{-1} \circ \bar{R}^{-1}$, where

$$\begin{aligned} h_1^{-1}(x, y) &= \begin{cases} (x, \arcsin(\frac{8y}{3\pi})) & \text{if } |y| \leq \frac{\pi}{4} \\ (x_c + \frac{x-x_c}{\tau}, \operatorname{sgn}(y) \arcsin(1 - \frac{\tau^2}{3})) & \text{if } \frac{\pi}{4} < |y| < \frac{\pi}{2} \\ (-\pi, \frac{\pi}{2}) & \text{else,} \end{cases} \\ \tau &= 2 - \frac{4|y|}{\pi} \\ x_c &= -\frac{3\pi}{4} + \frac{\pi}{2} \left\lfloor \frac{2(x + \pi)}{\pi} \right\rfloor \\ \bar{R}^{-1}(x, y) &= \left(\frac{x}{R}, \frac{y}{R} \right). \end{aligned}$$

These formulas come from [CR07].

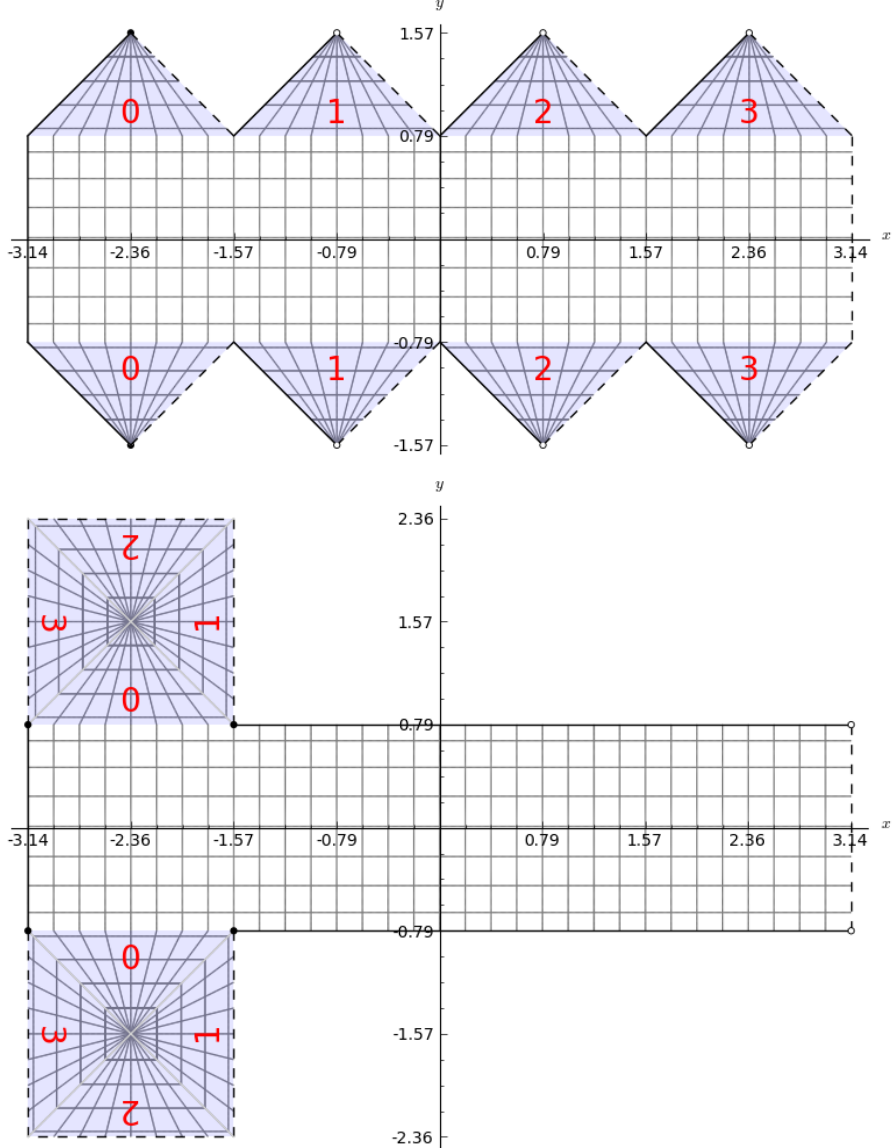


FIGURE 5. The (a) HEALPix and (b) $(0, 0)$ -rHEALPix projections of the unit sphere with a $\pi/16$ graticule.

A.2. Distortion of the Sphere. Every map projection necessarily distorts angles, lengths, or areas of the sphere [Eul78]. These distortions can be quantified by a map projection’s local scales, which we now compute for the HEALPix map projection according to [BS95, Section 1.6] and [Sny87, Section 4].

For this we need the partial derivatives of p and $h := h_R$ on the interior of D :

$$\begin{aligned}\frac{\partial p}{\partial \lambda} &= R(-\sin \lambda \cos \phi, \cos \lambda \cos \phi, 0) \\ \frac{\partial p}{\partial \phi} &= R(-\cos \lambda \sin \phi, -\sin \lambda \sin \phi, \cos \phi) \\ \frac{\partial h}{\partial \lambda} &= \begin{cases} R(1, 0) & \text{if } |\phi| \leq \phi_0 \\ R(\sigma, 0) & \text{else} \end{cases} \\ \frac{\partial h}{\partial \phi} &= \begin{cases} R(0, \frac{3\pi}{8} \cos \phi) & \text{if } |\phi| \leq \phi_0 \\ R(-\operatorname{sgn}(\phi)(\lambda - \lambda_c)(\frac{3}{2\sigma}) \cos \phi, \frac{3\pi}{8\sigma} \cos \phi) & \text{else.} \end{cases}\end{aligned}$$

Notice that $\partial p / \partial \lambda$ and $\partial p / \partial \phi$ are orthogonal since their dot product is 1. Notice also that $\cos \phi / \sigma$ tends to $\sqrt{2/3}$ as $|\phi|$ approaches $\pi/2$.

The local linear scale of a map projection at a given point and in a given direction is the reciprocal of the ratio of the length of an infinitesimal segment on the sphere to the length of the projected segment in the plane. The HEALPix local linear scales along parallels of latitude and meridians of longitude, respectively, are

$$\begin{aligned}s_P &= \left| \frac{\partial h}{\partial \lambda} \right| \left| \frac{\partial p}{\partial \lambda} \right|^{-1} = \left| \frac{\partial h}{\partial \lambda} \right| \frac{1}{R \cos \phi} = \frac{1}{\cos \phi} \begin{cases} 1 & \text{if } |\phi| \leq \phi_0 \\ \sigma & \text{else} \end{cases} \\ s_M &= \left| \frac{\partial h}{\partial \phi} \right| \left| \frac{\partial p}{\partial \phi} \right|^{-1} = \left| \frac{\partial h}{\partial \phi} \right| \frac{1}{R} = \frac{3\pi}{8} \cos \phi \begin{cases} 1 & \text{if } |\phi| \leq \phi_0 \\ \frac{1}{\sigma} \sqrt{(\lambda - \lambda_c)^2 \frac{16}{\pi^2} + 1} & \text{else.} \end{cases}\end{aligned}$$

Here $|(a, b)|$ denotes the Euclidean norm $\sqrt{a^2 + b^2}$.

The local area scale of a map projection at a point is the reciprocal of the ratio of the area of an infinitesimal parallelogram on the sphere to the area of its projection on the plane. For HEALPix this scale is

$$s_A = Jh(\lambda, \phi) \left| \frac{\partial p}{\partial \lambda} \times \frac{\partial p}{\partial \phi} \right|^{-1} = \frac{Jh(\lambda, \phi)}{|\partial p / \partial \lambda| |\partial p / \partial \phi|} = \frac{(3\pi/8)R^2 \cos \phi}{(R \cos \phi)R} = \frac{3\pi}{8},$$

where $Jh(\lambda, \phi)$ denotes the Jacobian determinant of $h(\lambda, \phi)$. Since a map projection is equiareal if and only if s_A is constant, we see that the HEALPix map projection is indeed equiareal.

HEALPix is conformal at points satisfying $s_P = s_M$ and $\partial h / \partial \lambda \cdot \partial h / \partial \phi = 0$, namely at points with latitude $\phi = \pm \arccos(\sqrt{8/(3\pi)}) \approx \pm 22.88^\circ$. In other words, the angle between any pair of lines on the sphere intersecting at any of these points is preserved when projected to the plane.

Under a general map projection an infinitesimal circle on the sphere centered at a given point projects to an infinitesimal ellipse on the plane, called the Tissot ellipse of the point. The major and minor radii, A and B respectively, of the Tissot ellipse are related to the local scales above by two theorems of Apollonius on conjugate ellipse diameters:

$$s_P^2 + s_M^2 = A^2 + B^2, \quad s_A = AB.$$

Thus

$$A = \sqrt{s_P^2 + s_M^2 + 2s_A} + \sqrt{s_P^2 + s_M^2 - 2s_A}$$

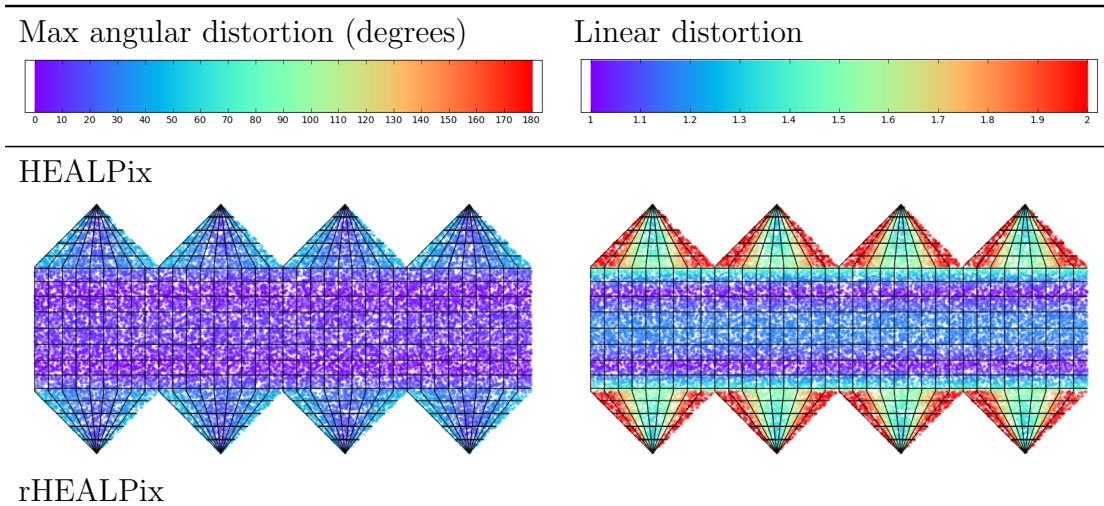
$$B = \sqrt{s_P^2 + s_M^2 + 2s_A} - \sqrt{s_P^2 + s_M^2 - 2s_A}.$$

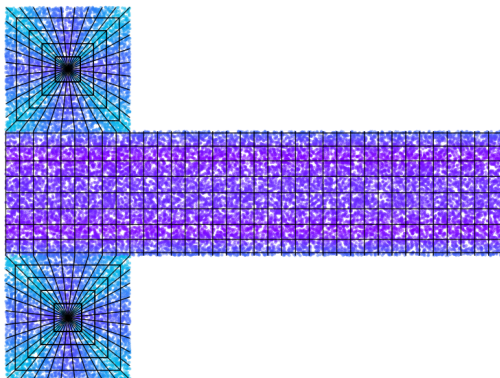
The radii of the Tissot ellipse at a point can be used to quantify a projection's local maximum angular distortion, local linear distortion, and local areal distortion at the point via the quantities

$$(\star) \quad 2 \arcsin \left(\frac{A - B}{A + B} \right), \quad \frac{A}{B}, \quad AB,$$

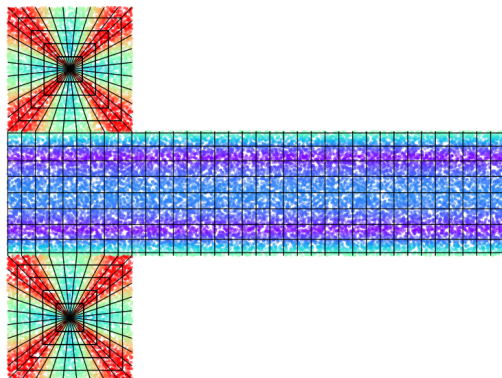
respectively. The first quantity is typically denoted by ω in cartographic texts, and $\omega/2$ is the greatest angular change a pair of perpendicular lines meeting at the given point on the ellipsoid undergo when projected onto the plane. For a conformal projection, this quantity is 0 (no angular distortion) at all points. The second quantity is the aspect ratio of the Tissot ellipse. For a conformal projection, this quantity is 1 (no linear distortion) at all points. The third quantity is the area of the bounding rectangle of the Tissot ellipse and also the local area scale. For an equiareal projection, this quantity is a single constant at all points. For an area-preserving projection, this quantity is 1 (no areal distortion) at all points.

Thus, reasonable measures of the global maximum angular distortion, global linear distortion, and global areal distortion of a map projection are the mean, standard deviation, minimum, maximum and median of the respective quantities (\star) . Table 2 presents sampling estimates of these measures for HEALPix and other map projections of the sphere of Earth mean radius 6,371,000 m (cf. [GG07]), and Table 3 presents several visualizations thereof. In particular, Table 3 demonstrates that the regions of greatest maximum angular and linear distortion for the (r)HEALPix projections lie around the left and right edges of the polar triangles.

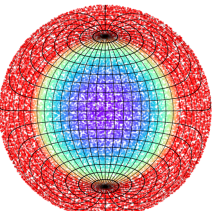
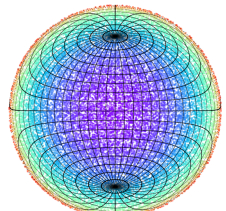




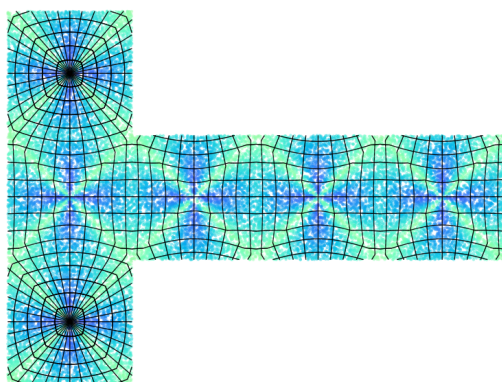
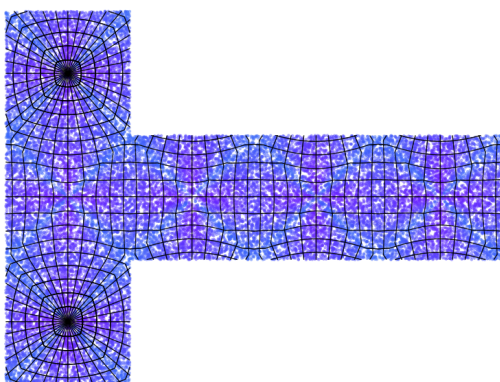
Lambert cylindrical equal area



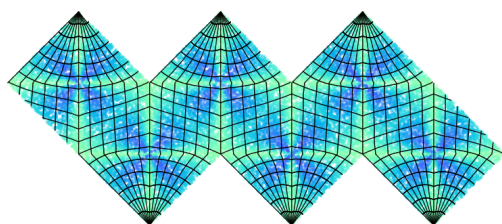
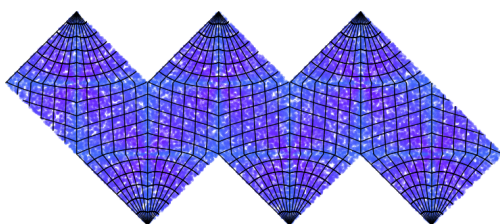
Lambert azimuthal equal area



Quadrilaterized spherical cube



Cubic Snyder equal area



Icosahedral Snyder equal area

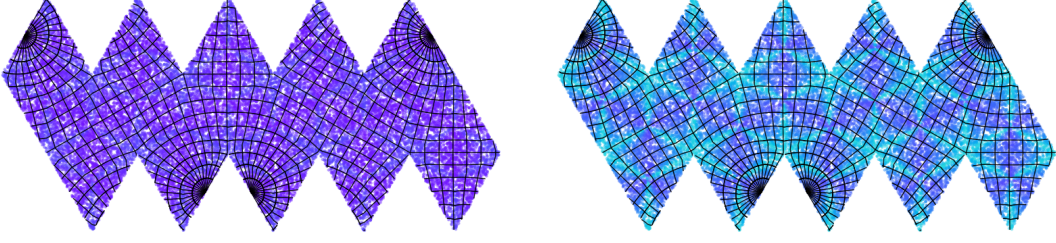


Table 3: Color-coded plots of the maximum angular distortion function $2 \arcsin((A - B)/(A + B))$ and the linear distortion function A/B of the equiareal projections, sphere, and number of sample points used in Table 2. Linear distortions values of 2 or more are all colored red.

A.3. Formulas for the Ellipsoid. Let $\mathbb{E}_{a,b}^2 \subset \mathbb{R}^3$ denote the ellipsoid of revolution centered at the origin with major radius a and minor radius b . For definiteness here, assume the ellipsoid is oblate, that is, it is generated by revolving an ellipse about its minor axis. By a map projection of the ellipsoid, we mean an injective function from $\mathbb{E}_{a,b}^2$ to the plane \mathbb{R}^2 . In cartography, points on the ellipsoid are usually described in terms of their longitude and geodetic latitude, that is, via the bijective parametrization $\hat{p} : D \rightarrow \mathbb{E}_{a,b}^2$ defined by

$$\hat{p}(\lambda, \phi) = (a \cos \lambda \cos \eta(\phi), a \sin \lambda \cos \eta(\phi), b \sin \eta(\phi)).$$

Here η is the parametric latitude of a point[¶], which can be expressed in terms of geodetic latitude via

$$\eta(\phi) = \begin{cases} \arctan(\sqrt{1 - e^2} \tan \phi) & \text{if } |\phi| \neq \frac{\pi}{2} \\ \phi & \text{else.} \end{cases}$$

Here $e = \sqrt{1 - (b/a)^2}$ is the eccentricity of the ellipsoid. Since $\tan \eta = \sqrt{(1 - e^2)} \tan \phi$ we have

$$\cos \eta = \frac{\cos \phi}{\sqrt{1 - e^2 \sin^2 \phi}}, \quad \sin \eta = \frac{\sqrt{1 - e^2} \sin \phi}{\sqrt{1 - e^2 \sin^2 \phi}}.$$

As in the spherical scenario, specifying a signature function $f : D \rightarrow \mathbb{R}^2$ uniquely determines a map projection $f \circ \hat{p}^{-1}$ of the ellipsoid.

As promised, we extend the HEALPix map projection to the ellipsoid $\mathbb{E}_{a,b}^2$ while preserving its features (i)–(iv) above. We do this in a way typical to equiareal map projections [Sny87, Section 3], namely, by applying the spherical version of the projection to the authalic sphere of the ellipsoid.

The authalic sphere $\mathbb{S}_{R_q}^2$ of the ellipsoid $\mathbb{E}_{a,b}^2$ is the unique sphere having the same area as the ellipsoid. The ellipsoid can be transformed into its authalic sphere via the area-preserving bijection $p \circ l \circ \hat{p}^{-1}$, where $l : D \rightarrow D$ is defined by

$$l(\lambda, \phi) = (\lambda, \beta(\phi)).$$

[¶] The geodetic latitude ϕ of a point X on $\mathbb{E}_{a,b}^2$ is the (smallest) angle between the equatorial plane and the line normal to $\mathbb{E}_{a,b}^2$ that passes through P . This line does *not* pass through the center of $\mathbb{E}_{a,b}^2$ when X is off the equator and poles.

The parametric latitude η of a point X on $\mathbb{E}_{a,b}^2$ is the (smallest) angle between the equatorial plane and the line normal to $\mathbb{E}_{a,b}^2$ that passes through X' , the vertical projection of X onto a surrounding sphere of radius a . This line always passes through the center of $\mathbb{E}_{a,b}^2$.

Map projection	Max angular distortion (degrees)						Linear distortion						Areal distortion						
	Mean	Std	Min	Max	Median	Mean	Std	Min	Max	Median	Mean	Std	Min	Max	Median	Min	Max	Median	
Equiareal projections																			
HEALPix	15.776	13.066	0.003	49.299	9.329	1.358	0.353	1.0	2.43	1.177	1.178	0.0	1.178	1.178	1.178	1.178	1.178	1.178	
rHEALPix	15.776	13.066	0.003	49.299	9.329	1.358	0.353	1.0	2.43	1.177	1.178	0.0	1.178	1.178	1.178	1.178	1.178	1.178	
Lambert cylindrical equal area	30.967	36.047	0.0	176.947	16.33	4.726	55.212	1.0	6364.621	1.33	1.0	0.0	1.0	1.0	1.0	1.0	1.0	1.0	
Lambert azimuthal equal area	49.099	39.746	0.0	178.885	38.831	10.842	213.924	1.0	30728.11	1.995	1.0	0.001	0.918	1.2	1.0	1.0	1.0	1.0	
Quadrilaterized spherical cube	16.161	4.467	6.44	25.141	15.883	1.332	0.105	1.119	1.556	1.321	1.178	0.0	1.178	1.178	1.178	1.178	1.178	1.178	
Cubic Snyder equal area	16.121	4.476	6.437	25.11	15.854	1.331	0.105	1.119	1.555	1.32	1.0	0.0	1.0	1.0	1.0	1.0	1.0	1.0	
Icosahedral Snyder equal area	9.541	3.141	4.878	17.234	8.831	1.183	0.066	1.089	1.352	1.167	1.0	0.0	1.0	1.0	1.0	1.0	1.0	1.0	
Conformal projections																			
Mercator	0.0	0.0	0.0	0.002	0.0	1.0	0.0	1.0	1.0	1.0	4.726	55.212	1.0	6364.621	1.33	1.33	1.33	1.33	
Stereographic	0.0	0.0	0.0	0.012	0.0	1.0	0.0	1.0	1.0	1.0	49995.603	6008139.487	1.0	1028684349.24	3.979	3.979	3.979	3.979	
Lambert conformal conic	0.0	0.0	0.0	0.004	0.0	1.0	0.0	1.0	1.0	1.0	386.307	35055.539	0.989	5736465.879	1.608	1.608	1.608	1.608	
Other projections																			
Equirectangular	16.873	21.612	0.0	153.663	8.186	1.547	1.527	1.0	79.78	1.153	1.547	1.527	1.0	79.78	1.153	1.153	1.153	1.153	
Azimuthal equidistant	33.508	28.685	0.0	169.198	25.584	2.459	4.097	1.0	280.216	1.568	2.459	4.099	1.0	280.431	1.568	1.568	1.568	1.568	
Winkel triple	23.283	14.423	0.176	143.5	19.414	1.579	0.631	1.003	29.469	1.402	1.052	0.44	0.44	0.818	22.938	0.97	0.97	0.97	0.97

TABLE 2. Sample mean, standard deviation, minimum, maximum, and median for the maximum angular distortion function $2 \arcsin((A - B)/(A + B))$, the linear distortion function A/B , and the areal distortion function AB for various common global map projections of the sphere of Earth mean radius 6,371,000 m. Here A and B denote the major and minor radii of the Tissot ellipse of a longitude-latitude point. We used a sample of 30,000 points chosen uniformly at random from the surface of the sphere (and not simply uniformly at random from the rectangle D). The sphere was decapitated at latitudes $\pm 89.5^\circ$, because some of the projections above are undefined at the poles.

Here β represents authalic latitude, which can be expressed in terms of geodetic latitude via

$$\begin{aligned}\beta(\phi) &= \arcsin\left(\frac{q(\phi)}{q(\pi/2)}\right) \\ q(\phi) &= \frac{(1-e^2)\sin\phi}{1-e^2\sin^2\phi} - \frac{1-e^2}{2e}\ln\left(\frac{1-e\sin\phi}{1+e\sin\phi}\right).\end{aligned}$$

Authalic latitude is slightly smaller in magnitude than geodetic latitude, but the two coincide at the poles and equator. The radius of the authalic sphere is $R_q = a\sqrt{q(\pi/2)/2}$.

Though l is a bijection, its inverse cannot be written in closed form. To calculate geodetic latitude ϕ approximately from authalic latitude β , it is common to use the truncated series approximation

$$\begin{aligned}\phi \approx \beta + &\left(\frac{1}{3}e^2 + \frac{31}{180}e^4 + \frac{517}{5040}e^6\right)\sin(2\beta) + \\ &\left(\frac{23}{360}e^4 + \frac{251}{3780}e^6\right)\sin(4\beta) + \frac{761}{45360}e^6\sin(6\beta).\end{aligned}$$

We define the signature function of the HEALPix map projection of the ellipsoid $\mathbb{E}_{a,b}^2$ to be $h_{R_q} \circ l$.

A.4. Distortion of the Ellipsoid. As for the sphere, to evaluate the distortion of the ellipsoid $\mathbb{E}_{a,b}^2$ under the HEALPix map projection we compute the projection's local scales. Let $h = h_{R_q}$. Because $h \circ l \circ \hat{p}^{-1} = (h \circ p^{-1}) \circ (p \circ l \circ \hat{p}^{-1})$ and the latter composite function preserves area, the local area scale is

$$\widehat{s_A} = s_A \cdot 1 = \frac{3\pi}{8}.$$

For the local linear scales we need the partial derivatives of \hat{p} , l , and h on the interior of D :

$$\begin{aligned}\frac{\partial \hat{p}}{\partial \lambda} &= (-a \sin \lambda \cos \eta, a \cos \lambda \cos \eta, 0) \\ \frac{\partial \hat{p}}{\partial \phi} &= \frac{d\eta}{d\phi}(-a \cos \lambda \sin \eta, -a \sin \lambda \sin \eta, b \cos \eta) \\ \frac{d\eta}{d\phi} &= \frac{\sqrt{1-e^2}}{1-e^2 \sin^2 \phi} \\ \frac{\partial l}{\partial \lambda} &= (1, 0) \\ \frac{\partial l}{\partial \phi} &= \left(0, \frac{d\beta}{d\phi}\right) \\ \frac{d\beta}{d\phi} &= \frac{|\partial \hat{p}/\partial \lambda| |\partial \hat{p}/\partial \phi|}{R_q^2 \cos \beta}.\end{aligned}$$

Notice that $\partial \hat{p}/\partial \lambda$ and $\partial \hat{p}/\partial \phi$ are orthogonal since their dot product is 1. The last equality follows from the fact that the local area scale of $p \circ l \circ \hat{p}^{-1}$ is

$$\begin{aligned}1 &= |\partial p/\partial \lambda \times \partial p/\partial \phi| Jl(\lambda, \phi) |\partial \hat{p}/\partial \lambda \times \partial \hat{p}/\partial \phi|^{-1} \\ &= R_q^2 \cos \beta (d\beta/d\phi) |\partial \hat{p}/\partial \lambda|^{-1} |\partial \hat{p}/\partial \phi|^{-1}.\end{aligned}$$

Using the derivatives above and $b^2 = a^2(1 - e^2)$ we get

$$\begin{aligned}\widehat{s_P} &= \left| \frac{\partial h}{\partial \lambda} \right| \left| \frac{\partial l}{\partial \lambda} \right| \left| \frac{\partial \widehat{p}}{\partial \lambda} \right|^{-1} = \left| \frac{\partial h}{\partial \lambda} \right| \frac{\sqrt{1 - e^2 \sin^2 \phi}}{a \cos \phi} \\ &= \frac{R_q \sqrt{1 - e^2 \sin^2 \phi}}{a \cos \phi} \begin{cases} 1 & \text{if } |\beta| \leq \phi_0 \\ \sigma & \text{else} \end{cases} \\ \widehat{s_M} &= \left| \frac{\partial h}{\partial \beta} \right| \left| \frac{\partial l}{\partial \phi} \right| \left| \frac{\partial \widehat{p}}{\partial \phi} \right|^{-1} = \left| \frac{\partial h}{\partial \beta} \right| \frac{d\beta}{d\phi} \left| \frac{\partial \widehat{p}}{\partial \phi} \right|^{-1} = \left| \frac{\partial h}{\partial \beta} \right| \frac{a \cos \phi}{R_q^2 \cos \beta \sqrt{1 - e^2 \sin^2 \phi}} \\ &= \frac{3\pi a \cos \phi}{8R_q \sqrt{1 - e^2 \sin^2 \phi}} \begin{cases} 1 & \text{if } |\beta| \leq \phi_0 \\ \frac{1}{\sigma} \sqrt{(\lambda - \lambda_c)^2 \frac{16}{\pi^2} + 1} & \text{else.} \end{cases}\end{aligned}$$

The HEALPix map projection of the ellipsoid is conformal at points satisfying $\widehat{s_P} = \widehat{s_M}$ and $\partial h / \partial \lambda \cdot \partial h / \partial \phi = 0$, that is, points for which $(3\pi/8)a^2 \cos^2 \phi = R_q^2(1 - e^2 \sin^2 \phi)$, that is, points at latitude $\phi \approx \pm 23.10^\circ$.

The formulas for the radii of the Tissot ellipses of the ellipsoid in terms of $\widehat{s_P}$, $\widehat{s_M}$, and $\widehat{s_A}$ are the same as for the sphere. Table 4 presents sampling estimates of the mean, standard deviation, minimum, maximum and median of A/B and AB on the WGS84 ellipsoid. We did not include the popular universal transverse Mercator (UTM) conformal map projection (or collection of projections) of the WGS84 ellipsoid, because, although it has approximately no linear or areal distortion on its domain, its domain is not really global, being restricted to latitudes south of $84^\circ N$ and north of $80^\circ S$.

APPENDIX B. THE rHEALPix MAP PROJECTION

The rHEALPix map projection was first described in passing in [CR07, Figure 5] and is the following simple rearrangement of the HEALPix map projection. Consider the image of the HEALPix map projection of the sphere or ellipsoid, number its north polar triangles 0–3 from east to west, and do the same for the south polar triangles; see Figure 1(a). Given integers $0 \leq n, s \leq 3$, combine the north polar triangles of the HEALPix map projection into a square upon north polar triangle n , and combine the south polar triangles into a square upon south polar triangle s . More specifically, rotate north polar triangle i by $(n+i) \bmod 4$ quarter turns counterclockwise about its center and translate it so that its former north tip lies on the north tip of triangle n , and rotate south polar triangle i by $(s+i) \bmod 4$ quarter turns clockwise about its center and translate it so that its former south tip lies on the south tip of triangle s . Call the result the (n, s) -rHEALPix map projection. For example, the $(1, 3)$ -rHEALPix map projection of the WGS84 ellipsoid is pictured in Figure 1(b).

Key features of the (n, s) -rHEALPix map projection are:

- (i) It is an equiareal map projection with area scaling factor $3\pi/8$ and low average angular and linear distortion.
- (ii) Parallels of latitude in the equatorial region (authalic latitudes of magnitude at most $\phi_0 := \arcsin(2/3) \approx 41.8^\circ$) project to horizontal lines and those in the polar (nonequatorial) region project to squares.
- (iii) The projection of a parallel of latitude uniformly divided is uniformly divided.
- (iv) Meridians of longitude project to vertical lines in the equatorial region and lines converging polewards in the polar region.

Map projection	Max angular distortion (degrees)					Linear distortion					Areal distortion				
	Mean	Std	Min	Max	Median	Mean	Std	Min	Max	Median	Mean	Std	Min	Max	Median
Equiareal projections															
HEALPix	15.651	12.993	0.002	49.329	9.386	1.36	0.352	1.0	2.428	1.178	1.178	0.0	1.178	1.178	1.178
rHEALPix	15.651	12.993	0.002	49.329	9.386	1.36	0.352	1.0	2.428	1.178	1.178	0.0	1.178	1.178	1.178
Lambert cylindrical equal area	30.597	35.817	0.0	177.669	16.268	4.954	66.078	1.0	5961.011	1.335	1.0	0.0	1.0	1.0	1.0
Lambert azimuthal equal area	48.813	39.741	0.0	178.364	38.386	11.306	198.871	1.0	18182.001	2.032	1.0	0.001	0.889	1.132	1.0
Quadrilaterized spherical cube	16.104	4.486	6.382	25.168	15.839	1.33	0.105	1.118	1.557	1.32	1.178	0.0	1.178	1.178	1.178
Cubic Snyder equal area	16.092	4.467	6.45	25.116	15.813	1.33	0.105	1.119	1.556	1.319	1.0	0.0	1.0	1.0	1.0
Icosahedral Snyder equal area	9.532	3.136	4.853	17.283	8.815	1.183	0.066	1.088	1.354	1.166	1.0	0.0	1.0	1.0	1.0
Conformal projections															
Mercator	0.0	0.0	0.0	0.003	0.0	1.0	0.0	1.0	1.0	4.954	66.078	1.0	5961.011	1.335	
Stereographic	0.0	0.0	0.0	0.005	0.0	1.0	0.0	1.0	1.0	148489.015	10765150.045	4.0	1341569280.88	16.512	
Lambert conformal conic	0.0	0.0	0.0	0.004	0.0	1.0	0.0	1.0	1.0	526.865	38526.357	0.989	5191993.371	1.603	
Other projections															
Equirectangular	16.592	21.569	0.0	156.982	8.034	1.546	1.604	1.0	77.338	1.153	1.548	1.597	1.003	77.08	1.158
Azimuthal equidistant	11.455	7.31	0.0	25.657	10.795	1.234	0.16	1.0	1.571	1.21	1.234	0.161	1.0	1.58	1.21
Winkel triple	23.231	14.376	0.249	145.781	19.296	1.585	0.702	1.002	39.228	1.412	1.053	0.424	0.821	19.729	0.972

TABLE 4. Sample mean, standard deviation, minimum, maximum, and median for the maximum angular distortion function $2 \arcsin((A - B)/(A + B))$, the linear distortion function A/B , and the areal distortion function AB for various common global map projections of the WGS84 ellipsoid. Here A and B denote the major and minor radii of the Tissot ellipse of a longitude-latitude point. We used a sample of 30,000 points chosen uniformly at random from the surface of the ellipsoid (and not simply uniformly at random from the rectangle D). The ellipsoid was decapitated at latitudes $\pm 89.5^\circ$, because some of the projections above are undefined at the poles.

- (v) The entire projection image can be divided into six isomorphic squares, four in the equatorial region and two in the polar region.

At first glance the (n, s) -rHEALPix map projection looks like the quadrilateralized spherical cube projections of [CO75, OL76], which are also equiareal map projections whose images can be divided into six isomorphic squares. However rHEALPix differs from these projections. For example, the edges of the six squares become meridians and parallels under the inverse rHEALPix projection, which is not the case for the other two projections.

B.1. rHEALPix Formulas for the Sphere and Ellipsoid. The signature functions of the (n, s) -rHEALPix map projection of the sphere \mathbb{S}_R^2 and the ellipsoid $\mathbb{E}_{a,b}^2$ are $g_{R,n,s} := \bar{R} \circ g_{1,n,s} \circ h_1$ and $g_{R_q,n,s} \circ l$ respectively, where $g_{1,n,s}$ is the area-preserving bijection that rearranges the polar triangles of the HEALPix map projection by rotation and translation:

$$g_{1,n,s}(x, y) = \begin{cases} M^{(c-n)}((x, y) - t_c) + \left(-\frac{3\pi}{4} + n\frac{\pi}{2}, \frac{\pi}{2}\right) & \text{if } y > \frac{\pi}{4} \\ M^{-(c-s)}((x, y) - t_c) + \left(-\frac{3\pi}{4} + s\frac{\pi}{2}, -\frac{\pi}{2}\right) & \text{if } y < -\frac{\pi}{4} \\ (x, y) & \text{else} \end{cases}$$

$$M = \begin{pmatrix} 0 & -1 \\ 1 & 0 \end{pmatrix}$$

$$c = \left\lfloor \frac{2(x + \pi)}{\pi} \right\rfloor$$

$$t_c = \left(-\frac{3\pi}{4} + c\frac{\pi}{2}, \operatorname{sgn}(y)\frac{\pi}{2} \right).$$

See Figure 5(b).

The inverse of $g_{1,n,s}$ is

$$g_{1,n,s}^{-1}(x, y) = \begin{cases} M^{-(c-n)}((x, y) - \left(-\frac{3\pi}{4} + n\frac{\pi}{2}, \frac{\pi}{2}\right)) + t_c & \text{if } y > \frac{\pi}{4} \\ M^{(c-s)}((x, y) - \left(-\frac{3\pi}{4} + s\frac{\pi}{2}, -\frac{\pi}{2}\right)) + t_c & \text{if } y < -\frac{\pi}{4} \\ (x, y) & \text{else,} \end{cases}$$

where this time the number c of the polar triangle that (x, y) lies in is defined by the following case statement. If $y > \frac{\pi}{4}$, then

$$c = \begin{cases} n \mod 4 & \text{if } y \leq L_1 \text{ and } y < L_2 \\ (n+1) \mod 4 & \text{if } y < L_1 \text{ and } y \geq L_2 \\ (n+2) \mod 4 & \text{if } y \geq L_1 \text{ and } y > L_2 \\ (n+3) \mod 4 & \text{else,} \end{cases}$$

where L_1 and L_2 are the y coordinates of the diagonals of the north polar square:

$$L_1 = x + \frac{3\pi}{4} - (n-1)\frac{\pi}{2}$$

$$L_2 = -x - \frac{3\pi}{4} + (n+1)\frac{\pi}{2};$$

if $y < -\frac{\pi}{4}$, then

$$c = \begin{cases} s \bmod 4 & \text{if } y > L_1 \text{ and } y \geq L_2 \\ (s+1) \bmod 4 & \text{if } y \leq L_1 \text{ and } y > L_2 \\ (s+2) \bmod 4 & \text{if } y < L_1 \text{ and } y \leq L_2 \\ (s+3) \bmod 4 & \text{else,} \end{cases}$$

where L_1 and L_2 are the y coordinates of the diagonals of the south polar square:

$$\begin{aligned} L_1 &= x + \frac{3\pi}{4} - (s+1)\frac{\pi}{2} \\ L_2 &= -x - \frac{3\pi}{4} + (s-1)\frac{\pi}{2}. \end{aligned}$$

Since an rHEALPix map projection is identical to the HEALPix map projection in the equatorial region, its spherical and ellipsoidal versions are also conformal at points with latitude $\approx \pm 22.88^\circ$ and $\approx \pm 23.10^\circ$, respectively.

Since the rHEALPix and HEALPix map projections are rigid transformations of each other, their local scales are identical at longitude-latitude points that map to the interiors of both projection images, which is almost all points, all points off a set of measure zero to be more precise. This fact is reflected statistically in identical entries in Tables 2 and 4 for the two projections.

LANDCARE RESEARCH, PRIVATE BAG 11052, MANAWATU MAIL CENTRE, PALMERSTON NORTH 4442, NEW ZEALAND

E-mail address: Gibbr@landcareresearch.co.nz

DEPARTMENT OF COMPUTER SCIENCE, UNIVERSITY OF AUCKLAND, PRIVATE BAG 92019, AUCKLAND 1001, NEW ZEALAND

E-mail address: raichev@cs.auckland.ac.nz

LANDCARE RESEARCH, PRIVATE BAG 11052, MANAWATU MAIL CENTRE, PALMERSTON NORTH 4442, NEW ZEALAND

E-mail address: SpethM@landcareresearch.co.nz